PART I

PHYSICS REQUIRED TO DESIGN LASER DIODES

P1: OSO c01 JWBS036-Numai

August 9, 2010

10:8

Printer Name: Yet to Come

1

ENERGY BANDS IN BULK AND QUANTUM STRUCTURES

1.1 INTRODUCTION

Transitions of Electrons

The **emission** and **absorption** of light are generated by the transitions of electrons. Light is emitted because electrons transit from high-energy states to lower-energy states, and light is absorbed in the reverse process. When electrons transit from high-energy states to lower-energy states, **nonradiative transitions**, which do not emit light, may exist as well as **radiative transitions**, which accompany light emissions.

Energy Bands

When the atomic spacing is so large that mutual interactions of atoms may be neglected, the electron energies are **discrete** and **energy levels** are formed. With a decrease in the atomic spacing, the positions of the electrons of neighboring atoms start to overlap. Therefore, the energy levels begin to split to satisfy the **Pauli exclusion principle**. With a further decrease in atomic spacing, the number of electrons whose positions overlap with each other increases. As a result, the number of split energy levels goes up, and the energy differences in the adjacent energy levels are reduced. In semiconductor crystals, the number of atoms per cubic centimeter is on the order of 10^{22} , where the atomic spacing is about 0.2 nm. As a result, the spacing of energy levels is much narrower than the **bandgap energy**, on the order of

electron volts. Therefore, the constituent energy levels are considered to be almost **continuous**, and **energy bands** are formed.

1.2 BULK STRUCTURE

Bulk

Semiconductors in which constituent atoms are placed periodically at a sufficiently long range compared with lattice spacing are called **bulk semiconductors**. In this section, the energy bands in bulk semiconductors are calculated.

$k \cdot p$ Perturbation

Semiconductors have free electrons and holes only in the vicinity of band edges. As a result, the band shapes and effective masses of carriers near band edges often give us sufficient information about optical transitions. To analyze the energy bands in the neighbor of band edges, $k \cdot p$ perturbation theory [1–4] is often employed. The wave functions and energies of the bands are calculated with $\Delta k = k - k_0$ as a perturbation parameter, where k is a wave vector near a band edge and k_0 is a wave vector at a band edge. For simplicity, $k_0 = 0$ is selected in the following.

Schrödinger Equation

The **Schrödinger equation** in the steady state is given by [5,6]

$$\left[-\frac{\hbar^2}{2m} \nabla^2 + V(\mathbf{r}) \right] \psi_n(\mathbf{k}, \mathbf{r}) = E_n(\mathbf{k}) \psi_n(\mathbf{k}, \mathbf{r}), \tag{1.1}$$

where $\hbar = h/2\pi = 1.0546 \times 10^{-34} \, \text{J} \cdot \text{s}$ is **Dirac's constant**, $h = 6.6261 \times 10^{-34} \, \text{J} \cdot \text{s}$ is **Planck's constant**, $m = 9.1094 \times 10^{-31} \, \text{kg}$ is the electron mass in vacuum, V(r) is a potential, $\psi_n(\boldsymbol{k}, \boldsymbol{r})$ is a wave function, $E_n(\boldsymbol{k})$ is an **energy eigenvalue**, n is a **quantum number**, and \boldsymbol{k} is a wave vector. In **single crystals** where the atoms are placed **periodically**, the potential V(r) is also spatially periodic. Therefore, as a solution of (1.1), we can consider a **Bloch function**, such as

$$\psi_n(\mathbf{k}, \mathbf{r}) = \exp(\mathrm{i}\,\mathbf{k} \cdot \mathbf{r}) u_n(\mathbf{k}, \mathbf{r}),\tag{1.2}$$

$$u_n(\mathbf{k}, \mathbf{r}) = u_n(\mathbf{k}, \mathbf{r} + \mathbf{R}), \tag{1.3}$$

where R is a translational vector which represents the periodicity of the crystal. Equations (1.2) and (1.3) constitute the **Bloch theorem**. Substituting (1.2) into (1.1)

5

$$\left[-\frac{\hbar^2}{2m} \nabla^2 + V(\mathbf{r}) + \mathcal{H}' \right] u_n(\mathbf{k}, \mathbf{r}) = E_n(\mathbf{k}) u_n(\mathbf{k}, \mathbf{r}), \tag{1.4}$$

where

$$\mathcal{H}' = \frac{\hbar^2 \mathbf{k}^2}{2m} + \frac{\hbar}{m} \mathbf{k} \cdot \mathbf{p},\tag{1.5}$$

$$\mathbf{p} = -\mathrm{i}\,\hbar\nabla.\tag{1.6}$$

Note that the $k \cdot p$ perturbation theory, whose name is derived from the second term on the right-hand side of (1.5), is valid only for small k, and we solve (1.4) by regarding (1.5) as the **perturbation**.

First-Order Perturbation Theory

For an energy band with n = 0, the wave equation for an unperturbed state with k = 0 is expressed as

$$\left[-\frac{\hbar^2}{2m} \nabla^2 + V(\mathbf{r}) \right] u_0(0, \mathbf{r}) = E_0(0) u_0(0, \mathbf{r}). \tag{1.7}$$

In the following, for simplicity, the energy $E_0(0)$ is represented as E_0 .

In **first-order perturbation theory**, the wave function $u_0(k, r)$ for a nondegenerate case is given by

$$u_0(\mathbf{k}, \mathbf{r}) = u_0(0, \mathbf{r}) + \sum_{\alpha \neq 0} \frac{-i \left(\hbar^2 / m\right) \mathbf{k} \cdot \langle \alpha | \nabla | 0 \rangle}{E_0 - E_\alpha} u_\alpha(0, \mathbf{r}), \tag{1.8}$$

$$\langle \alpha | \nabla | 0 \rangle = \int u_{\alpha}^{*}(0, \mathbf{r}) \nabla u_{0}(0, \mathbf{r}) \, \mathrm{d}^{3} \mathbf{r}. \tag{1.9}$$

Here $u_0(\mathbf{k}, \mathbf{r})$ and $u_\alpha(\mathbf{k}, \mathbf{r})$ are assumed to be orthonormal functions and $\langle \alpha |$ and $|0\rangle$ are the **bra** and **ket** vectors, respectively, which were introduced by Dirac.

Second-Order Perturbation Theory

In **second-order perturbation theory**, an energy eigenvalue is obtained as

$$E(\mathbf{k}) = E_0 + \frac{\hbar^2 k^2}{2m} + \frac{\hbar^2}{m^2} \sum_{i,j} k_i k_j \sum_{\alpha \neq 0} \frac{\langle 0 | p_i | \alpha \rangle \langle \alpha | p_j | 0 \rangle}{E_0 - E_\alpha}.$$
 (1.10)

The reciprocal effective mass tensor is defined as

$$\left(\frac{1}{m}\right)_{ij} \equiv \frac{1}{\hbar^2} \frac{\partial^2 E}{\partial k_i \partial k_j} = \frac{1}{m} \left(\delta_{ij} + \frac{2}{m} \sum_{\alpha \neq 0} \frac{\langle 0 | p_i | \alpha \rangle \langle \alpha | p_j | 0 \rangle}{E_0 - E_\alpha}\right).$$
(1.11)

Using (1.11), (1.10) is reduced to

$$E(\mathbf{k}) = E_0 + \frac{\hbar^2}{2} \sum_{i,j} \left(\frac{1}{m}\right)_{ij} k_i k_j.$$
 (1.12)

Equations (1.11) and (1.12) indicate that the effect of the periodic potential of the crystal is included in the effective mass of the electron, which makes analysis easier. In a cyclotron resonance experiment, the rest mass in vacuum in not measured, but the effective mass is measured.

sp³ Hybrid Orbitals

Next, we consider the energy bands of semiconductor crystals with **zinc blende structures**, which are used widely as material for light sources. In zinc blende structures, the atomic bonds are formed via sp^3 **hybrid orbitals**. Therefore, the wave functions for electrons in zinc blende or diamond structures are expressed as superpositions of s- and p-orbital functions.

We assume that the bottom of a conduction band and the tops of valence bands are placed at k = 0, as in direct transition semiconductors. When spin-orbit interaction is neglected, the tops of the valence bands are threefold **degenerate**, corresponding to the three p-orbitals (p_x, p_y, p_z) . Here the s-orbital wave function for the bottom of the conduction band is $u_s(\mathbf{r})$, and the p-orbital wave functions for the tops of the valence bands are $u_x = xf(\mathbf{r})$, $u_y = yf(\mathbf{r})$, and $u_z = zf(\mathbf{r})$, where $f(\mathbf{r})$ is a spherical function.

Since the energy bands are degenerate, a perturbed wave equation is given by a linear superposition of $u_s(\mathbf{r})$ and $u_j(\mathbf{r})$ (j = x, y, z), such as

$$u_n(\mathbf{k}, \mathbf{r}) = Au_s(\mathbf{r}) + Bu_x(\mathbf{r}) + Cu_y(\mathbf{r}) + Du_z(\mathbf{r}), \tag{1.13}$$

where A, B, C, and D are coefficients.

To obtain the energy eigenvalues, (1.4) is rewritten

$$\left[-\frac{\hbar^2}{2m} \nabla^2 + V(\mathbf{r}) + \mathcal{H}'_{\mathrm{d}} \right] u_n(\mathbf{k}, \mathbf{r}) = \left[E_n(\mathbf{k}) - \frac{\hbar^2 k^2}{2m} \right] u_n(\mathbf{k}, \mathbf{r}), \tag{1.14}$$

$$\mathcal{H}'_{d} = \frac{\hbar}{m} \, \mathbf{k} \cdot \mathbf{p} = -\frac{\mathrm{i} \, \hbar^2}{m} \mathbf{k} \cdot \nabla. \tag{1.15}$$

By setting k = 0 in (1.14), an unperturbed equation is obtained. For a conduction band, we set $E_n(0) = E_c$, which is the energy of the bottom of a conduction band, and $u_0(0, \mathbf{r}) = u_s(\mathbf{r})$; for valence bands, we set $E_n(0) = E_v$, which is the energy of the top of each valence band, and $u_0(0, \mathbf{r}) = u_j(\mathbf{r})$ (j = x, y, z).

Substituting (1.13) into (1.14); multiplying $u_s^*(\mathbf{r})$, $u_x^*(\mathbf{r})$, $u_y^*(\mathbf{r})$, and $u_z^*(\mathbf{r})$ from the left-hand side; and then integrating with respect to a volume over the space leads to

$$(\mathcal{H}'_{ss} + E_{c} - \lambda)A + \mathcal{H}'_{sx}B + \mathcal{H}'_{sy}C + \mathcal{H}'_{sz}D = 0,
\mathcal{H}'_{xs}A + (\mathcal{H}'_{xx} + E_{v} - \lambda)B + \mathcal{H}'_{xy}C + \mathcal{H}'_{xz}D = 0,
\mathcal{H}'_{ys}A + \mathcal{H}'_{yx}B + (\mathcal{H}'_{yy} + E_{v} - \lambda)C + \mathcal{H}'_{yz}D = 0,
\mathcal{H}'_{zs}A + \mathcal{H}'_{zx}B + \mathcal{H}'_{zy}C + (\mathcal{H}'_{zz} + E_{v} - \lambda)D = 0,$$
(1.16)

Printer Name: Yet to Come

where

$$\mathcal{H}'_{ij} = \langle u_i | \mathcal{H}'_{d} | u_j \rangle = \int u_i^*(\mathbf{r}) \mathcal{H}'_{d} u_j(\mathbf{r}) d^3 \mathbf{r} \qquad (i, j = s, x, y, z), \qquad (1.17)$$

$$\lambda = E_n(\mathbf{k}) - \frac{\hbar^2 k^2}{2m}.\tag{1.18}$$

Note that the orthonormality of $u_s(\mathbf{r})$ and $u_j(\mathbf{r})$ (j = x, y, z) was used to derive (1.16).

The condition used to obtain solutions A, B, C, and D other than A = B = C = D = 0 is

$$\begin{vmatrix}
E_{c} - \lambda & Pk_{x} & Pk_{y} & Pk_{z} \\
P^{*}k_{x} & E_{v} - \lambda & 0 & 0 \\
P^{*}k_{y} & 0 & E_{v} - \lambda & 0 \\
P^{*}k_{z} & 0 & 0 & E_{v} - \lambda
\end{vmatrix} = 0,$$
(1.19)

where

$$P = -i\frac{\hbar^2}{m} \int u_s^* \frac{\partial u_j}{\partial r_j} d^3 \mathbf{r}, \quad P^* = -i\frac{\hbar^2}{m} \int u_j^* \frac{\partial u_s}{\partial r_j} d^3 \mathbf{r}$$

$$(j = x, y, z, \quad r_x = x, \quad r_y = y, \quad r_z = z). \tag{1.20}$$

From (1.19) we obtain

$$E_{1,2}(\mathbf{k}) = \frac{E_{\rm c} + E_{\rm v}}{2} + \frac{\hbar^2 k^2}{2m} \pm \left[\left(\frac{E_{\rm c} - E_{\rm v}}{2} \right)^2 + k^2 |P|^2 \right]^{1/2},\tag{1.21}$$

$$E_{3,4}(\mathbf{k}) = E_{\rm v} + \frac{\hbar^2 k^2}{2m},\tag{1.22}$$

where (1.18) was used.

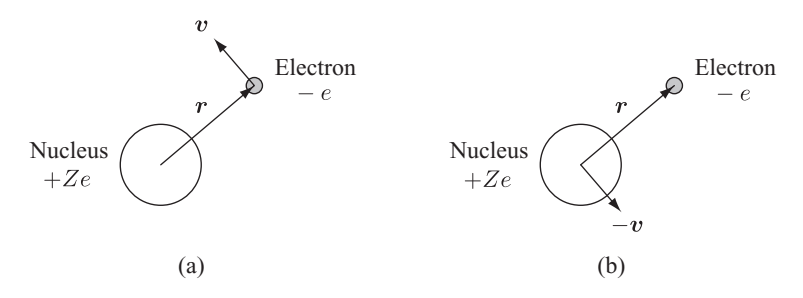


FIGURE 1.1 Motions of an electron.

Spin-Orbit Interaction

In addition to $k \cdot p$ perturbation, we consider spin-orbit interaction and second-order perturbation. First, let us consider **spin-orbit interaction** semiclassically. As shown in Fig. 1(a), an electron with electric charge $-e = -1.6022 \times 10^{-19}$ C rotates about the nucleus with electric charge +Ze. The velocity of the electron is v and the position vector of the electron is r, with the position of the nucleus as the initial point.

If we see the nucleus from the electron as shown in Fig. 1.1(b), the nucleus seems to rotate about the electron with a velocity -v. As a result, a **magnetic flux density** B is produced at the position of the electron, which is written

$$\mathbf{B} = \frac{\mu_0}{4\pi} Ze \frac{\mathbf{r} \times \mathbf{v}}{r^3} = \frac{\mu_0}{4\pi} \frac{Ze}{m} \frac{1}{r^3} \mathbf{l}. \tag{1.23}$$

This equation is known as **Biot–Savart's law**. In (1.23), μ_0 is magnetic permeability of vacuum, and l is the **orbital angular momentum**, which is given by

$$l = r \times p = r \times mv. \tag{1.24}$$

The spin magnetic moment μ_s is expressed as

$$\mu_{\rm s} = -\frac{e}{m}s = -\frac{2\mu_{\rm B}}{\hbar}s,\tag{1.25}$$

where s is the **spin angular momentum** and μ_B is the **Bohr magneton**, which is defined as

$$\mu_{\rm B} \equiv \frac{e\hbar}{2m} = 9.2732 \times 10^{-24} \,\mathrm{A \cdot m^2}.$$
 (1.26)

As a result, the magnetic field, which is generated at the position of the electron due to the orbital motions of the nucleus, interacts with the electron's spin magnetic moment. The **interaction energy** \mathcal{H}_{SO} between the magnetic flux density \boldsymbol{B} and the

spin magnetic moment μ_s is obtained as

$$\mathcal{H}_{SO} = -\boldsymbol{\mu}_{s} \cdot \boldsymbol{B} = \frac{\mu_{0}}{4\pi} \frac{Ze^{2}}{m^{2}} \frac{1}{r^{3}} \boldsymbol{l} \cdot \boldsymbol{s}. \tag{1.27}$$

Printer Name: Yet to Come

Note that (1.27) is obtained using classical electromagnetism.

From Dirac's **relativistic quantum mechanics**, the interaction energy \mathcal{H}_{SO} is given by

$$\mathcal{H}_{SO} = \frac{\mu_0}{4\pi} \frac{Ze^2}{2m^2} \frac{1}{r^3} \boldsymbol{l} \cdot \boldsymbol{s}, \tag{1.28}$$

which is half of (1.27).

Pauli's Spin Matrices

Pauli's spin matrices σ are defined as

$$s = \frac{\hbar}{2} \sigma, \tag{1.29}$$

$$\sigma_x = \begin{bmatrix} 0 & 1 \\ 1 & 0 \end{bmatrix}, \quad \sigma_y = \begin{bmatrix} 0 & -i \\ i & 0 \end{bmatrix}, \quad \sigma_z = \begin{bmatrix} 1 & 0 \\ 0 & -1 \end{bmatrix}.$$
 (1.30)

Using Pauli's spin matrices, the **spin-orbit interaction Hamiltonian** \mathcal{H}_{SO} can be rewritten

$$\mathcal{H}_{SO} = \frac{\mu_0}{4\pi} \frac{Ze^2}{2m^2} \frac{1}{r^3} \frac{\hbar}{2} \mathbf{l} \cdot \mathbf{\sigma}. \tag{1.31}$$

If the **up-spin** \uparrow ($s_z = \hbar/2$) and **down-spin** \downarrow ($s_z = -\hbar/2$) are expressed as α and β , respectively, they are written in matrix form:

$$\alpha = \begin{bmatrix} 1 \\ 0 \end{bmatrix}, \quad \beta = \begin{bmatrix} 0 \\ 1 \end{bmatrix}. \tag{1.32}$$

As a result, operations of σ_z on α and β are written

$$\sigma_z \alpha = \alpha, \quad \sigma_z \beta = -\beta.$$
 (1.33)

When a **spherical polar coordinate system** is used, the spin-orbit interaction Hamiltonian \mathcal{H}_{SO} is expressed as

$$\mathcal{H}_{SO} = \frac{\hbar}{2} \, \xi(\mathbf{r}) \, \mathbf{l} \cdot \mathbf{\sigma} = \frac{\hbar}{2} \, \xi(\mathbf{r}) \left(l_z \sigma_z + \frac{l_+ \sigma_- + l_- \sigma_+}{2} \right), \tag{1.34}$$

where

$$\xi(\mathbf{r}) = \frac{\mu_0}{4\pi} \frac{Ze^2}{2m^2} \frac{1}{r^3},$$

$$l_{+} = l_x + i l_y, \quad l_{-} = l_x - i l_y,$$

$$\sigma_{+} = \sigma_x + i \sigma_y, \quad \sigma_{-} = \sigma_x - i \sigma_y.$$
(1.35)

When the spin-orbit interaction Hamiltonian \mathcal{H}_{SO} is added to (1.14) as a perturbation term, the Schrödinger equation is written

$$\left[-\frac{\hbar^2}{2m} \nabla^2 + V(\mathbf{r}) + \mathcal{H}'_{d} + \mathcal{H}_{SO} \right] u_n(\mathbf{k}, \mathbf{r}) = \left[E_n(\mathbf{k}) - \frac{\hbar^2 k^2}{2m} \right] u_n(\mathbf{k}, \mathbf{r}). \quad (1.36)$$

It should be noted that l operates on $\exp(i \mathbf{k} \cdot \mathbf{r})$ in the Bloch function, but this operation is neglected because the result is much smaller than the other terms.

To solve (1.36), the wave functions are represented in the spherical polar coordinate system as

$$u_s = u_s, \ u_+ = -\frac{u_x + u_y}{\sqrt{2}} \sim -\frac{x + y}{\sqrt{2}}, \ u_- = \frac{u_x - u_y}{\sqrt{2}} \sim \frac{x - y}{\sqrt{2}}, \ u_z \sim z.$$
 (1.37)

In (1.37), the spherical function f(r) is omitted after \sim to simplify expressions. Note that $\sqrt{2}$ is introduced in the denominators to normalize the wave functions. Using the spherical harmonic function Y_1^m , the wave functions u_+ , u_- , and u_z are expressed as

$$u_{+} = Y_{1}^{1} = -\frac{1}{2}\sqrt{\frac{3}{2\pi}} \frac{x + iy}{\sqrt{x^{2} + y^{2} + z^{2}}} = -\frac{1}{2}\sqrt{\frac{3}{2\pi}} \exp(i\phi) \sin\theta,$$

$$u_{-} = Y_{1}^{-1} = \frac{1}{2}\sqrt{\frac{3}{2\pi}} \frac{x - iy}{\sqrt{x^{2} + y^{2} + z^{2}}} = \frac{1}{2}\sqrt{\frac{3}{2\pi}} \exp(-i\phi) \sin\theta,$$

$$u_{z} = Y_{1}^{0} = \frac{1}{2}\sqrt{\frac{3}{\pi}} \frac{z}{\sqrt{x^{2} + y^{2} + z^{2}}} = \frac{1}{2}\sqrt{\frac{3}{\pi}} \cos\theta,$$
(1.38)

where $x = r \sin \theta \cos \phi$, $y = r \sin \theta \sin \phi$, and $z = r \cos \theta$.

Including the up- and down-spins α and β , the following eight wave functions are present:

$$u_s\alpha$$
, $u_s\beta$, $u_+\alpha$, $u_+\beta$, $u_z\alpha$, $u_z\beta$, $u_-\alpha$, $u_-\beta$.

Therefore, we have to calculate the elements of the 8×8 matrix to obtain energy eigenvalues from (1.36).

For brevity, we assume that $\mathbf{k} = (k_x, k_y, k_z)$ is a vector in the positive direction of the z-axis and express the elements of \mathbf{k} as

$$k_z = k, \quad k_x = k_y = 0.$$
 (1.39)

In this case we only have to solve the determinant for the 4×4 matrix on four elements of $u_s\alpha$, $u_+\beta$, $u_z\alpha$, $u_-\beta$ or those of $u_s\beta$, $u_-\alpha$, $u_z\beta$, $u_+\alpha$ because of the symmetry in the 8×8 matrix. This determinant for the 4×4 matrix is written

$$\begin{vmatrix} E_{c} - \lambda & 0 & Pk & 0 \\ 0 & E_{v} - \lambda - \frac{\Delta_{0}}{3} & \frac{\sqrt{2}}{3} \Delta_{0} & 0 \\ P^{*}k & \frac{\sqrt{2}}{3} \Delta_{0} & E_{v} - \lambda & 0 \\ 0 & 0 & 0 & E_{v} - \lambda + \frac{\Delta_{0}}{3} \end{vmatrix} = 0, \quad (1.40)$$

where the terms including Δ_0 are the matrix elements of \mathcal{H}_{SO} , and the other terms are those of \mathcal{H}'_d . Here, using $\xi(\mathbf{r})$ in (1.35), Δ_0 is expressed as

$$\frac{\Delta_0}{3} = \frac{\hbar^2}{2} \int u_+^* u_+ \xi(\mathbf{r}) \, \mathrm{d}^3 \mathbf{r} = \frac{\hbar^2}{2} \int u_-^* u_- \xi(\mathbf{r}) \, \mathrm{d}^3 \mathbf{r}
= \frac{\hbar^2}{4} \int (u_x^2 + u_y^2) \xi(\mathbf{r}) \, \mathrm{d}^3 \mathbf{r} = \frac{\hbar^2}{2} \int u_z^2 \xi(\mathbf{r}) \, \mathrm{d}^3 \mathbf{r}.$$
(1.41)

From (1.40), the energy of valence band 1 is obtained as

$$E_{\rm vl}(\mathbf{k}) = E_{\rm v} + \frac{\Delta_0}{3} + \frac{\hbar^2 k^2}{2m}.$$
 (1.42)

When $|P|^2k^2$ is small enough, the energy of the conduction band E_c is reduced to

$$E_{c}(\mathbf{k}) = E_{c} + \frac{\hbar^{2} k^{2}}{2m} + \frac{|P|^{2} k^{2}}{3} \left(\frac{2}{E_{\sigma}} + \frac{1}{E_{\sigma} + \Delta_{0}} \right), \tag{1.43}$$

where

$$E_{\rm g} = E_{\rm c} - E_{\rm v} - \frac{\Delta_0}{3}.\tag{1.44}$$

Similarly, the energies of valence bands 2 and 3 are given by

$$E_{v2}(\mathbf{k}) = E_{v} + \frac{\Delta_{0}}{3} + \frac{\hbar^{2}k^{2}}{2m} - \frac{2|P|^{2}k^{2}}{3E_{g}},$$
(1.45)

$$E_{v3}(\mathbf{k}) = E_{v} - \frac{2}{3}\Delta_{0} + \frac{\hbar^{2}k^{2}}{2m} - \frac{|P|^{2}k^{2}}{3(E_{g} + \Delta_{0})}.$$
 (1.46)

Note that these results were obtained under first-order $k \cdot p$ perturbation.

Valence Bands

Under second-order perturbation, the energies of the valence bands are given by

$$E_{v1,2}(\mathbf{k}) = E_v + \frac{\Delta_0}{3} + A_2 k^2$$

$$\pm \left[B_2^2 k^4 + C_2^2 \left(k_x^2 k_y^2 + k_y^2 k_z^2 + k_z^2 k_x^2 \right) \right]^{1/2} \quad (1 \to +, 2 \to -), \tag{1.47}$$

$$E_{v3}(\mathbf{k}) = E_{v} - \frac{2}{3}\Delta_{0} + A_{2}k^{2}. \tag{1.48}$$

Equations (1.43), (1.47), and (1.48) are shown in Fig. 1.2. From the definition of effective mass in (1.11), the band with energy $E_{v1}(\mathbf{k})$ is referred to as a **heavy hole band** and that with $E_{v2}(\mathbf{k})$ is called a **light hole band**. It should be noted that the heavy and light hole bands are degenerate at $\mathbf{k} = 0$. The band with energy $E_{v3}(\mathbf{k})$ is called the **split-off band**, and Δ_0 is called the **split-off energy**. The coefficients A_2 , B_2 , and C_2 in (1.47) and (1.48) are determined experimentally by **cyclotron**

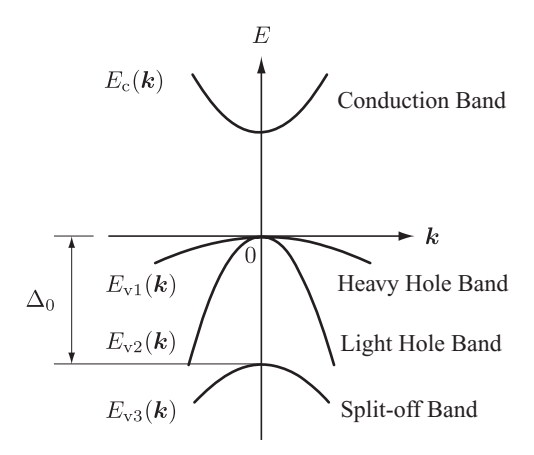


FIGURE 1.2 Energy bands of a bulk structure when the spin-orbit interaction is considered under a second-order perturbation.

TABLE 1.1 Relations Between Operators and Eigenvalues

Operator	Eigenvalue
l^2	$l(l+1)\hbar^2$ ($l=0$:s-orbital, $l=1$:p-orbitals)
l_z	$m_l \hbar, \ m_l = 1, 0, -1$
s^2	$s(s+1)\hbar^2, \ s=1/2$
S_z	$m_s \hbar, \ m_s = 1/2, -1/2$
$\frac{s_z}{m{j}^2}$	$j(j+1)\hbar^2$, $j=3/2,1/2$
j_z	$m_j\hbar$, $m_{j=3/2} = 3/2$, $1/2$, $-1/2$, $-3/2$, $m_{j=1/2} = 1/2$, $-1/2$

resonance. In general, the effective masses depend on the direction of k, and the energy bands are more complicated.

Note that in the preceding analysis, the energy bands of **direct transition semi-conductors**, in which the bottom of the conduction band and the tops of the valence bands are placed at k = 0, are calculated. In **indirect transition**, the k's of the bottom of the conduction band and the k's of the tops of the valence bands are different.

Due to the spin-orbit interaction, the quantum states are indicated by j = l + s, where l is the angular momentum operator and s is the spin operator. Therefore, as indexes of the wave functions, we can use the quantum numbers j and m_j , which represent the eigenvalues of operators j and j_z , respectively. The relations between the operators and the eigenvalues are summarized in Table 1.1.

When we express the wave functions as $|j, m_j\rangle$, the wave functions of the valence bands under the second-order perturbation are expressed as follows:

For a heavy hole band,

$$\left| \frac{3}{2}, \frac{3}{2} \right\rangle = \frac{1}{\sqrt{2}} \left| (x + i y)\alpha \right\rangle,$$

$$\left| \frac{3}{2}, -\frac{3}{2} \right\rangle = \frac{1}{\sqrt{2}} \left| (x - i y)\beta \right\rangle,$$
(1.49)

for a light hole band,

$$\left| \frac{3}{2}, \frac{1}{2} \right\rangle = \frac{1}{\sqrt{6}} \left| 2z\alpha + (x + iy)\beta \right\rangle,$$

$$\left| \frac{3}{2}, -\frac{1}{2} \right\rangle = \frac{1}{\sqrt{6}} \left| 2z\beta - (x - iy)\alpha \right\rangle,$$
(1.50)

and for a split-off band,

$$\left|\frac{1}{2}, \frac{1}{2}\right\rangle = \frac{1}{\sqrt{3}} |z\alpha - (x + iy)\beta\rangle,$$

$$\left|\frac{1}{2}, -\frac{1}{2}\right\rangle = \frac{1}{\sqrt{3}} |z\beta + (x - iy)\alpha\rangle.$$
(1.51)

1.3 QUANTUM STRUCTURES

Quantum Effects

Semiconductor structures whose sizes are small enough that their **quantum effects**, such as splitting of energy bands and the tunneling effect, may be significant are called **quantum structures**.

Square Well

Electrons in quantum structures feel both the **periodic potential** of crystals and the quantum well potential. First, the energy eigenvalues and wave functions of a particle in a square well potential are reviewed briefly. As shown in Fig. 1.3, we assume that a carrier is present in a square potential well V(r) as

$$V(\mathbf{r}) = \begin{cases} 0 & \text{inside the well,} \\ \infty & \text{at the boundaries} \end{cases}$$
 (1.52)

When the potential well is a cube with side L, the boundary conditions for a wave function $\varphi(x, y, z)$ are given by

$$\varphi(0, y, z) = \varphi(L, y, z) = 0,
\varphi(x, 0, z) = \varphi(x, L, z) = 0,
\varphi(x, y, 0) = \varphi(x, y, L) = 0.$$
(1.53)

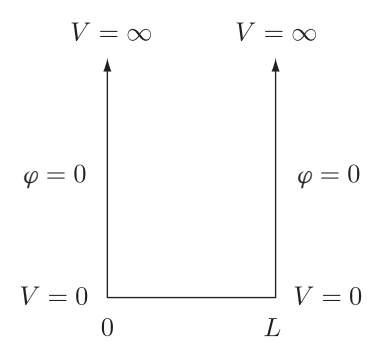


FIGURE 1.3 Square well potential.

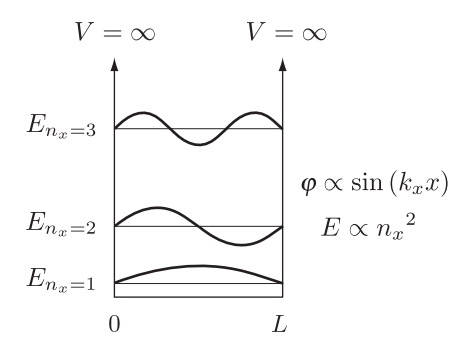


FIGURE 1.4 Wave function φ and energy eigenvalues E in a one-dimensional square well potential.

Under these boundary conditions, the wave function $\varphi(x, y, z)$ and energy eigenvalue E are obtained as

$$\varphi(x, y, z) = \sqrt{\frac{8}{L^3}} \sin k_x x \cdot \sin k_y y \cdot \sin k_z z,$$

$$E = \frac{\hbar^2}{2m} (k_x^2 + k_y^2 + k_z^2),$$

$$k_x = \frac{n_x \pi}{L}, \ k_y = \frac{n_y \pi}{L}, \ k_z = \frac{n_z \pi}{L} \quad (n_x, n_y, n_z = 1, 2, 3, \ldots).$$
(1.54)

Figure 1.4 shows the wave function φ and energy eigenvalues E for a one-dimensional square well potential. The energy eigenvalues E are **discrete** and their values are proportional to a square of the quantum number n_x . In addition, with a decrease in L, the energy separation between the energy levels increases.

Potential Well and Energy Barrier

Figure 1.5 shows the energies of the conduction band and valence bands at k=0 for GaAs, which is sandwiched by AlGaAs layers. The low-energy regions for electrons in the conduction band and holes in the valence bands are called **potential wells**. Note that in Fig. 1.5, the vertical line shows the energy of the electrons, and the energy of the holes decreases with an increase in the height of the vertical line. When the width of the potential well L_z is on the order of less than several tens of nanometers, the potential well is called the **quantum well**. The bandgaps of AlGaAs layers are higher than those of GaAs. As a result, these AlGaAs layers become the energy barriers for GaAs and are called **energy barrier layers**. At the interfaces of the quantum well and the barriers, energy differences exist in the conduction band ΔE_c , and in the valence bands, ΔE_v , and are called **band offsets**.

Printer Name: Yet to Come

16 ENERGY BANDS IN BULK AND QUANTUM STRUCTURES

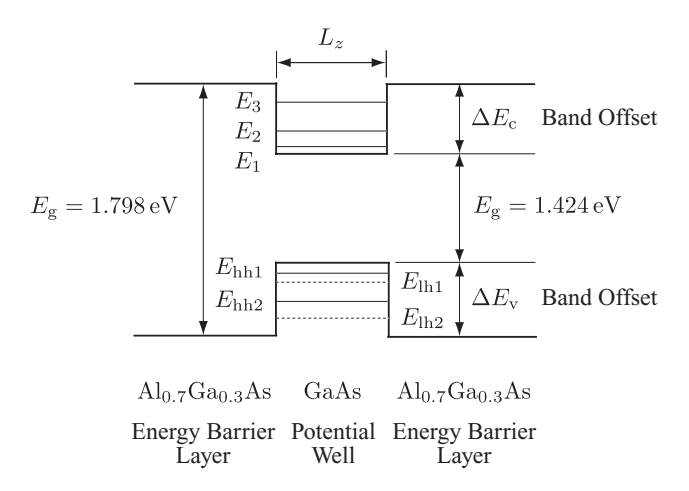


FIGURE 1.5 Quantum well structure.

Effective Mass Approximation

The periods of the potential for semiconductor crystals are represented by lattice constants which are on the order of 0.5 nm. In contrast, the thickness of potential wells or barriers in quantum structures is between an order of nanometers and that of several tens of nanometers. Hence, in quantum structures, electrons and holes feel both **periodic** and **quantum potentials**. If we use **effective mass**, the effect of the periodic potential is included in the effective mass, as shown in (1.12), and we only have to consider the quantum potential, referred to as the **effective mass approximation**.

Under effective mass approximation, a wave function in the quantum structure is obtained as a product of **base function** ψ and **envelope function** φ .

As base function ψ we use a wave function for the periodic potential:

$$\psi_n(\mathbf{k}, \mathbf{r}) = \exp(\mathrm{i}\,\mathbf{k} \cdot \mathbf{r}) u_{nk}(\mathbf{r}), \quad u_n(\mathbf{k}, \mathbf{r}) = u_{nk}(\mathbf{r} + \mathbf{R}). \tag{1.55}$$

As the envelope function φ , we use a wave function for the quantum potential. For example, for a cube with a side length of L and infinite potential at the boundaries, the envelope function φ is given by

$$\varphi(x, y, z) = \sqrt{\frac{8}{L^3}} \sin k_x x \cdot \sin k_y y \cdot \sin k_z z.$$
 (1.56)

Figure 1.6 shows one-, two-, and three-dimensional quantum wells. A sheet in which only L_z is of quantum size, as shown in Fig. 1.6(a), is called a **one-dimensional quantum well** or simply, a quantum well. A stripe in which only L_y and L_z are quantum sizes, as shown in Fig. 1.6(b), is called a **two-dimensional quantum well**

QUANTUM STRUCTURES

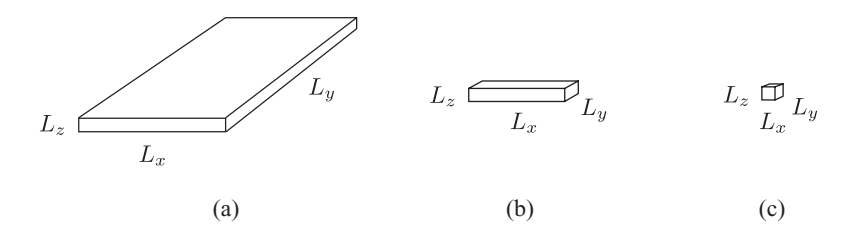


FIGURE 1.6 (a) One-, (b) two-, and (c) three-dimensional quantum wells.

or a **quantum wire**. A box whose L_x , L_y , and L_z are all quantum sizes, as shown in Fig. 1.6(c), is called a **three-dimensional quantum well** or a **quantum box**.

The energies of the carriers, which are confined completely in the sheet shown in Fig. 1.6(a), are written

$$E = E_{xy} + E_z,$$

$$E_{xy} = \frac{\hbar^2}{2m^*} \frac{\pi^2}{L^2} (n_x^2 + n_y^2), \quad E_z = \frac{\hbar^2}{2m^*} \frac{\pi^2}{L_z^2} n_z^2,$$
(1.57)

Printer Name: Yet to Come

where \hbar is Dirac's constant; m^* is the effective mass of the carrier; and n_x , n_y , and n_z are quantum numbers. If n_x , n_y , and n_z are of the same order, we have $E_{xy} \ll E_z$.

Density of States

As an example, let us calculate the **density of states** in a one-dimensional quantum well for $n_z = 1$. The density of states is determined by the number of combinations of n_x and n_y . When n_x and n_y are large enough, the combinations (n_x, n_y) for constant energy E_{xy} are represented by the points on the circumference of a circle with radius r, which is given by

$$r^{2} = n_{x}^{2} + n_{y}^{2} = \frac{2m^{*}L^{2}}{\hbar^{2}\pi^{2}}E_{xy}.$$
 (1.58)

Because both n_x and n_y are positive numbers, the number S of combinations (n_x, n_y) is given by the area of a quarter circle with radius r. As a result, S is expressed as

$$S = \frac{1}{4}\pi r^2 = \frac{\pi}{4}(n_x^2 + n_y^2) = \frac{\pi}{4}\frac{2m^*L^2}{\hbar^2\pi^2}E_{xy} = \frac{m^*L^2}{2\hbar^2\pi}E_{xy}.$$
 (1.59)

Considering the up- and down-spins, the number of states N is twice as large as S, which is written

$$N = 2S = \frac{m^* L^2}{\hbar^2 \pi} E_{xy}.$$
 (1.60)

Substituting $E_{xy} = E - E_{z=1}$ into (1.60), the electron concentration n for the energy between zero and E is obtained as

$$n = \frac{N}{L^2 L_z} = \frac{m^*}{\hbar^2 \pi L_z} (E - E_{z=1}). \tag{1.61}$$

When we define the density of states per volume for the energy between E and E + dE as $\rho_1(E)$, we have

$$\int \rho_1(E) \, \mathrm{d}E \equiv n. \tag{1.62}$$

From (1.61) and (1.62), we obtain

$$\rho_1(E) \equiv \frac{\mathrm{d}n}{\mathrm{d}E} = \frac{m^*}{\hbar^2 \pi L_z}.$$
 (1.63)

The densities of states for $n_z=2,3,\ldots$ are calculated similarly, and the results are shown in Fig. 1.7(a). Here L_z is $3 \text{ nm}; m^*$ is 0.08m, where m is the electron mass in vacuum; and the $\rho_1(E)$ for $n_z=1, 2$, and 3 are indicated as ρ_{11}, ρ_{12} , and ρ_{13} , respectively. It should be noted that the density of states for a one-dimensional quantum well is a **step function**. In contrast, the bulk structures have a density of states such that

$$\rho_0(E) = \frac{(2m^*)^{3/2}}{2\pi^2 \hbar^3} E^{1/2},\tag{1.64}$$

which is proportional to $E^{1/2}$ as shown by a dashed line, because the number of states is represented by the number of the points existing in one-eighth of a sphere with radius r.

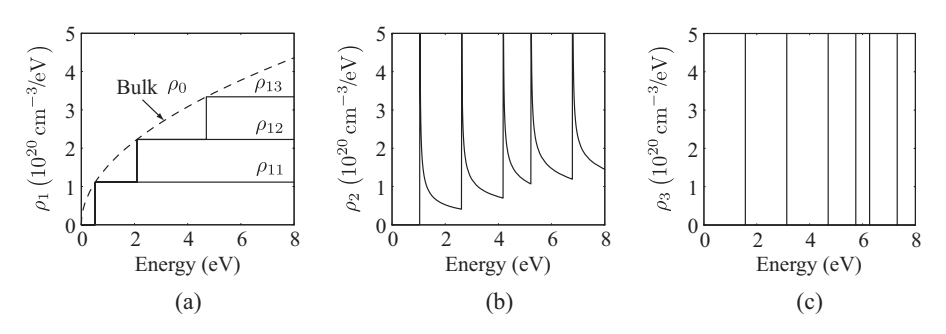


FIGURE 1.7 Density of states for (a) one-, (b) two-, and (c) three-dimensional quantum wells.

If we set $L_y = L_z = L$, the energies of the carriers, which are confined completely in the wire shown in Fig. 1.6(b), are written

$$E = E_x + E_{yz},$$

$$E_x = \frac{\hbar^2}{2m^*} \frac{\pi^2}{L_x^2} n_x^2, \quad E_{yz} = \frac{\hbar^2}{2m^*} \frac{\pi^2}{L^2} (n_y^2 + n_z^2).$$
(1.65)

For a pair of quantum numbers (n_v, n_z) , the density of states $\rho_2(E)$ is obtained as

$$\rho_2(E) = \frac{\sqrt{2m^*}}{\hbar\pi L^2} E_x^{-1/2} = \frac{\sqrt{2m^*}}{\hbar\pi L^2} (E - E_{yz})^{-1/2}.$$
 (1.66)

The result calculated for (1.66) is shown in Fig. 1.7(b). When the energy E is equal to E_{yz} , the density of states $\rho_2(E)$ is infinity. When E exceeds E_{yz} , $\rho_2(E)$ decreases in proportion to $(E - E_{yz})^{-1/2}$, which leads to a density of states $\rho_2(E)$ with a sawtoothed shape.

If we set $L_x = L_y = L_z = L$, the energies of the carriers, which are confined completely in the box shown in Fig. 1.6 (c), are written

$$E = E_x + E_y + E_z,$$

$$E_x = \frac{\hbar^2}{2m^*} \frac{\pi^2}{L^2} n_x^2, \quad E_y = \frac{\hbar^2}{2m^*} \frac{\pi^2}{L^2} n_y^2, \quad E_z = \frac{\hbar^2}{2m^*} \frac{\pi^2}{L^2} n_z^2.$$
(1.67)

It should be noted that the energy eigenvalues are completely discrete. The density of states $\rho_3(E)$ is a **delta function**, which is written

$$\rho_3(E) = 2\sum_{n_x, n_y, n_z} \delta(E - E_x - E_y - E_z). \tag{1.68}$$

Figure 1.7(c) shows the number of states per volume and the density of states in a three-dimensional quantum well.

With an increase in the dimension of the quantum wells, the energy bandwidths of the densities of states decrease. Therefore, the energy distribution of the electron concentrations narrows with an increase in the dimension of the quantum wells, as shown in Fig. 1.8. Therefore, the optical gain concentrates on a certain energy (wavelength). As a result, in quantum well lasers, a low threshold current, a high speed modulation, low chirping, and a narrow spectral linewidth are expected.

1.4 SUPERLATTICES

Array quantum structures and solitary structures are called **superlattices**. From the viewpoint of the potential, superlattices are classified as follows. Figure 1.9 shows three kinds of potentials of superlattices. The horizontal direction indicates the position of the layers, and the vertical direction represents the energy of the electrons.

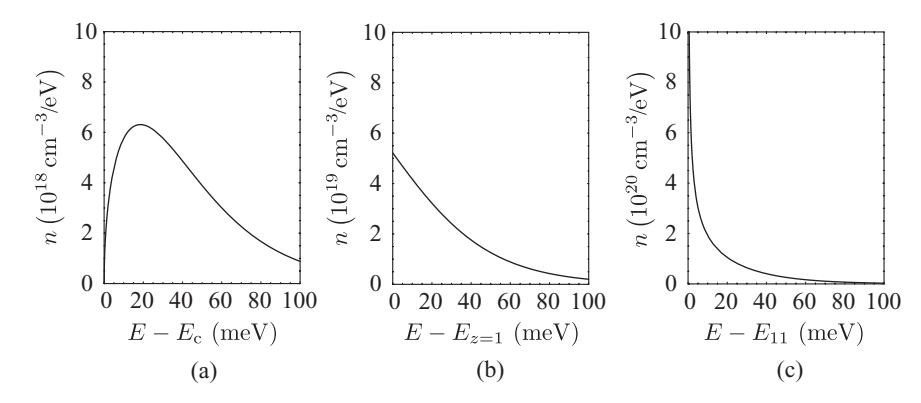


FIGURE 1.8 Energy distribution of electron concentrations in quantum wells: (a) bulk structure; (b) one-dimensional quantum; (c) two-dimensional quantum structure.

With an increase in height, the energy of electrons increases and that of holes decreases. As shown in Fig. 1.9(a), in a **type I superlattice**, the position of the potential well for electrons in the conduction band is the same as that for holes in the valence band. Therefore, both electrons and holes are confined in semiconductor layer B, which has a narrower bandgap than that of semiconductor layer A. In the **type II superlattice** in Fig. 1.9(b), the electrons in the conduction band are confined in semiconductor layer B, and the holes in the valence band are confined in semiconductor layer A. In the **type III superlattice** in Fig. 1.9(c), the energy of the conduction band of semiconductor layer B overlaps that of the valence band of semiconductor layer A, which results in a **semimetal**. Note that in the literature, types II and III are sometimes called types I' and II, respectively.

From the perspective of the period, superlattices are classified as follows. Figure 1.10 shows the relationships between the characteristics of superlattices and the thickness of barriers and wells. When each layer thickness is larger than several tens of nanometers, only the bulk characteristics are observed. If the barrier thickness is less than several tens of nanometers, the **quantum mechanical tunneling effect** appears. When the barriers are thick and only the wells are thin, quantum energy levels are formed in the wells. If such wells are used as the active layers in light-

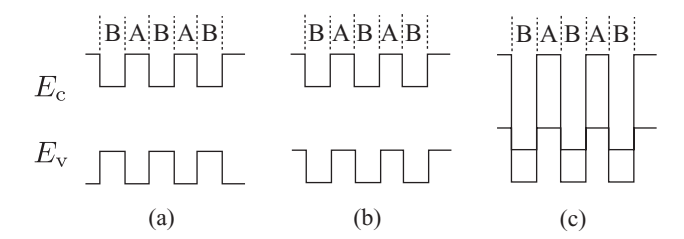


FIGURE 1.9 Classification of super lattices by potential: (a) type I; (b) type II; and (c) type III.

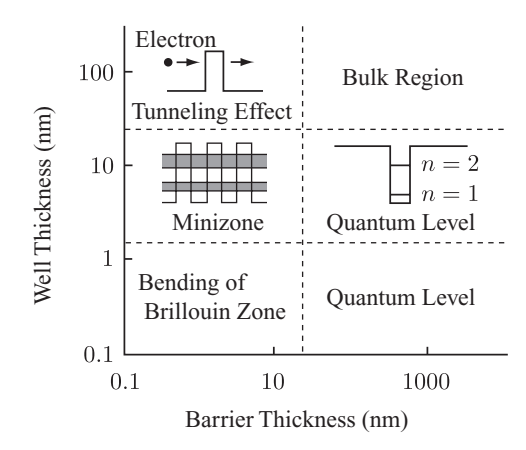


FIGURE 1.10 Classification of superlattices by period.

emitting devices, narrow light emission spectra are obtained. When both barriers and wells are thinner than about 10 nm, the wave functions of a well start to penetrate adjacent wells. As a result, the wave functions of each well overlap each other, which produces **minizones** and induces **Bloch oscillations** or **negative resistances**. When the thickness of both barriers and wells decreases further, down to the order of atomic layers, **bending of Brillouin zones** appears, which will transform indirect transition materials into direct transition materials.

REFERENCES

- 1. E. O. Kane, "Band structure of indium antimonide," J. Phys. Chem. Solids 1, 249 (1957).
- 2. C. Kittel, Quantum Theory of Solids, 2nd ed., Wiley, New York, 1987.
- G. Bastard, Wave Mechanics Applied to Semiconductor Heterostructures, Halsted Press, New York, 1988.
- 4. S. Datta, Quantum Phenomena, Addison-Wesley, Reading, MA, 1989.
- 5. L. I. Schiff, Quantum Mechanics, 3rd ed., McGraw-Hill, New York, 1968.
- 6. A. Messiah, Quantum Mechanics, Vols.1 and 2, North-Holland, Amsterdam, 1961.
- 7. T. Numai, Fundamentals of Semiconductor Lasers, Springer-Verlag, New York, 2004.

P1: OSO c01 JWBS036-Numai

August 9, 2010

10:8

Printer Name: Yet to Come